

# Rosmarinic Acid Prevents Radiation-Induced Pulmonary Fibrosis Through Attenuation of ROS/MYPT1/TGF $\beta$ 1 Signaling Via miR-19b-3p

Tingting Zhang<sup>1</sup> , Shanshan Ma<sup>1</sup>, Chang Liu<sup>1</sup> , Kai Hu<sup>1</sup>, Meng Xu<sup>1</sup> and Rensheng Wang<sup>1</sup>

## Abstract

The mechanism of pulmonary fibrosis caused by irradiation remains obscure. Since rosmarinic acid (RA) have anti-oxidant and anti-inflammatory properties, we aimed to evaluate the effect of RA on the X-ray-induced lung injury. Male rats received RA (30, 60, or 120 mg/kg) 7 days before 15 Gy of X-ray irradiation. Here, we showed that RA reduced X-ray-induced the expression of inflammatory related factors, and the level of reactive oxygen species. RA down-regulated the phosphorylation of nuclear factor kappa-B (NF- $\kappa$ B). We found that thoracic tumor patients whose lung regions received radiation showed lower level of microRNA-19b-3p (miR-19b-3p). Furthermore, we provided evidence that miR-19b-3p targets myosin phosphatase target subunit 1 (MYPT1), and RA attenuated RhoA/Rock signaling through upregulating miR-19b-3p, leading to the inhibition of fibrosis. In conclusion, RA may be an effective agent to relieve the pulmonary fibrosis caused by radiotherapy of thoracic tumor.

## Keywords

irradiation, rosmarinic acid, pulmonary fibrosis, miR-19b-3p

## Introduction

At present, radiotherapy is one of the main treatment methods, in nearly two-thirds of cancer patients, alone or more commonly combined with surgery and chemotherapy to treat a variety of cancer.<sup>1</sup> Many factors, including the biological characteristics of tumor and normal tissue, the regimen of radiotherapy, the physical condition of patients and radiation toxicity, contribute to the clinical outcome after radiotherapy. Radiotherapy will inevitably cause radiation damage to normal tissues surrounding tumor, which may affect and even threaten the patient's quality of life.<sup>2</sup> Radiation damage to the lung usually occurs in patients undergoing radiotherapy with chest tumors such as lung cancer, breast cancer, esophageal cancer and other malignant tumors. Radiation pneumonia is usually observed in the early stage, and then develops into radiation-induced pulmonary fibrosis in the late-stage.<sup>3,4</sup>

Accumulating evidence revealed that inflammation of the lung activates diverse signaling pathways, including nuclear factor kappa-B (NF- $\kappa$ B) and RhoA/Rho kinase pathway.<sup>5,6</sup> Well-characterized functions of NF- $\kappa$ B pathway include the regulation of inflammation and immunity.<sup>7</sup> TNF- $\alpha$ -induced

NF- $\kappa$ B activation exacerbates bleomycin-induced pulmonary fibrosis and salidroside have been shown to be involved in the protection of bleomycin-induced pulmonary fibrosis by activating Nrf2 signaling and in inhibiting NF- $\kappa$ B pathway.<sup>8</sup> Reactive oxygen species (ROS) plays an important role in radiation injury. It can lead to DNA damage and lipid peroxidation, thus initiating a series of cascade effects of the inflammatory response and gene activation, and finally further leading to tissue damage.<sup>9,10</sup> Angiotensin II (AngII) induced lung fibroblast migration and  $\alpha$ -collagen I synthesis through upregulating

<sup>1</sup> Department of Radiation Oncology, The First Affiliated Hospital of Guangxi Medical University, Nanning, China

Received 22 November 2019; received revised 15 September 2020; accepted 28 September 2020

## Corresponding Author:

Rensheng Wang, Department of Radiation Oncology, The First Affiliated Hospital of Guangxi Medical University, No. 6 Shuangyong Road, Nanning 530021, China.

Email: 13807806008@163.com



ROS-mediated RhoA/Rock pathway, suggesting that ROS/RhoA axis is involved in the pulmonary fibrosis.<sup>11</sup>

MicroRNAs (miRNAs), a class of 17–23 nucleotide non-coding RNAs, have been documented to be involved in diverse biological and pathological processes by binding to 3'-UTR (3'-untranslated region) of the target mRNAs, thus inducing the translational inhibition and degradation of mRNAs.<sup>12</sup> MicroRNA-19b-3p (miR-19b-3p) has been implicated in cell survival, proliferation, and metastasis in cancer cells.<sup>13,14</sup> However, the role of miR-19b-3p in irradiation-induced fibrosis is still unclear.

Rosmarinic acid (RA) is a kind of acid-containing polyphenol hydroxyl, which widely exists in many kinds of plants, and has many pharmacological effects such as antibacterial, antiviral, antioxidant and anti-inflammatory.<sup>15</sup> Earlier studies have shown that RA suppresses dextran sulphate sodium (DSS)-induced inflammation via dual inhibition of NF- $\kappa$ B and STAT3 activation.<sup>16</sup>

Lipopolysaccharide-induced neuroinflammatory responses was mitigated in the present of RA.<sup>17</sup> However, the function of RA in radiation-induced inflammation and fibrosis remains poorly elucidated. In the present study, we investigated the relationship between RA and X-ray-induced pulmonary fibrosis and clarified the possibly influenced mechanisms.

## Materials and Methods

### Patient Samples

Serum samples from 30 patients with thoracic tumor patients with pre- and post-radiotherapy were collected from the First Affiliated Hospital of Guangxi Medical University, Nanning, China. All patients participating in this study had signed the informed consent prior to their inclusion in the study. The experimental study and the collection of patient's serum for the study were approved by the First Affiliated Hospital of Guangxi Medical University Ethical Review Committee. The study was conducted in accordance with the Declaration of Helsinki.

### Ethics Statement

All animal experiments were performed according to the recommendations of the Committee on the Ethics of Animal Experiments of Guangxi Medical University (permit no. 201711015).

### Animals and Radiation Exposure

40 Male Sprague Dawley (SD) rats (210–250 g; 9 weeks old) were randomly divided into 5 groups. Rats in irradiation (IR) group and control (Ctrl) group were subjected with irradiation or sham irradiation at the lung regions. Rats in experimental groups were treated with irradiation and the increasing doses of RA (30, 60, or 120 mg/kg) 7 days intragastrically before irradiation until sacrificed. RA was purchased from Shanghai Yuan-ye Biotechnology Co., Ltd. (Shanghai, China) and dissolved

in physiological saline. All rats were fixed to a plane board after being anesthetized. The lung regions of rats in the IR group and experimental groups were positioned under simulation computerized tomography (Brilliance CT Big Bore, Philips Medical Systems, Cleveland, OHIO), and then received a single dose of 15 Gy of X-ray by a linear accelerator (Varian Clinac iX, Varian Medical Systems Inc, Palo Alto, CA) with other parts of the body shielded.

### Cell Culture and Transfection

The IMR-90 cells (a human embryonic lung fibroblasts cell line) were obtained from ATCC, and routinely cultured in DMEM medium (Gibco, Grand Island, NY) supplemented with 10% fetal bovine serum (Gibco) and 1% penicillin-streptomycin at 37°C. IMR-90 cells were plated in 6-well plates and transfected with miRNAs employing Lipofectamine RNAiMAX Transfection Reagent (Invitrogen, Carlsbad, CA) according to the manufacturer's instructions. The miR-19b-3p inhibitor (5'-AGUCAAAACGUACCUAAACGUGU-3') and negative control (5'-CUCCACUGCUUCACUUGACUA-3') Oligonucleotides were purchased from Sangon Biotech Shanghai.

### Sample Collection and Enzyme-Linked Immunoassay (ELISA) Analysis

Lung tissues of rats were resected under anesthesia. Per 8 rats in each group were randomly sacrificed at 30 days postirradiation. Blood was collected through the abdominal aorta. Subsequently, the serum was separated by centrifugation (3,500 rpm/min, 10 min, 4 °C). Serum Inflammation-related cytokines level was analyzed using available ELISA kit: IL-6 (R&D, Sao paulo, MN, USA); IL-2 (R&D); TNF- $\alpha$  (R&D).

### Messenger Ribonucleic Acid (mRNA) Analysis

Total RNA was extracted using TRIzol reagent according to the manufacturer's instructions (Invitrogen). cDNA was synthesized with PrimeScripTMRT Master Mix cDNA synthesis system (Takara, Japan). TB GreenTM Premix EX TaqTM II (Takara) was used for quantification. Expression of the gene of interest was normalized to the  $\beta$ -actin RNA level (mRNA) or U6 RNA level (miRNA). The following primers were used for RT-PCR:  $\beta$ -actin (forward 5'-CGTAAA GACCTCTATGCAACA-3'; reverse 5'-TAGGAGCCAGGGCAGTAATC-3'), MCP-1 (forward 5'-ATACTGGTCTGTTGTGGGTG-3'; reverse 5'-TGCCTTCTGGGAC-3'), RANTES (forward 5'-GGCCACCACGCTCTTCTGTC-3'; reverse 5'-GGGCTACGGGCTTGT CACTC-3'). ICAM-1 (forward 5'-TCTGCAGCGTG TGTGGATT-3'; reverse 5'-GGCTCATCATCGAATTGGCAC-3'). MiR-19b-3p (forward 5'-TGTGCAAATCCATGCAAAACTG-3'; reverse 5'-CAGTGCGTGT CGTGGAGT-3'). U6 (forward 5'-CTCGCTTCGGCAGCAC-3'; reverse 5'-AACGCTTCACGAATTTGCGT-3').

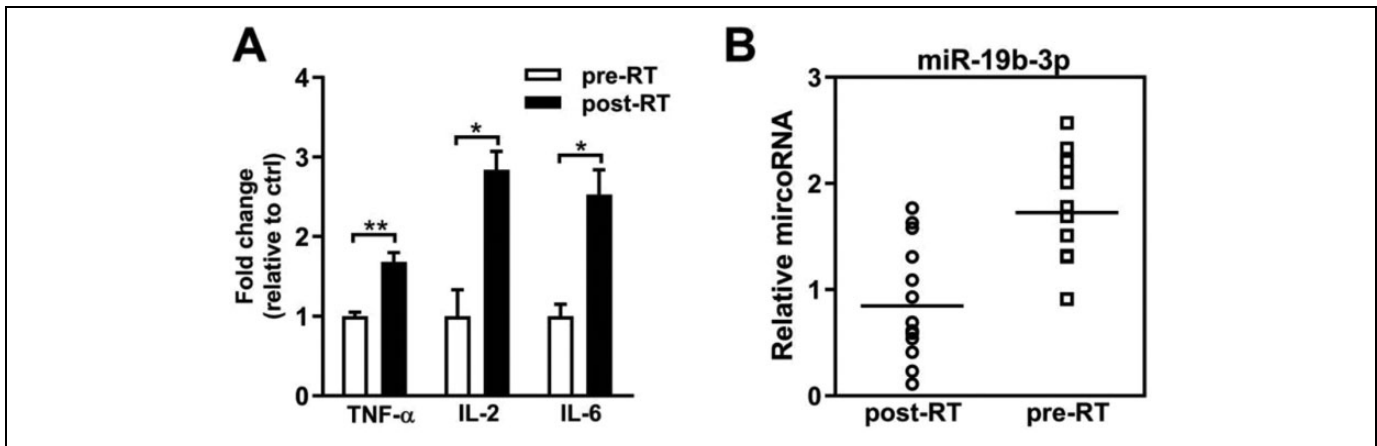


**Figure 1.** The miR-19b-3p is downregulated in radiotherapy. A, The expression levels of TNF- $\alpha$ , IL-2, and IL-6 in serum of the patients with thoracic tumors were detected by ELISA assay. B, The expression levels of miR-19b-3p in serum of the patients with thoracic tumors were detected by qPCR. Data are represented as the mean  $\pm$  SEM. ANOVA was performed to analyze the differences (\* $P < 0.05$ ; \*\* $P < 0.01$  in comparison with the indicated group). Abbreviation: pre-RT, pre-radiotherapy; post-RT, post-radiotherapy; TNF- $\alpha$ : Tumor necrosis factor- $\alpha$ ; IL-6: interleukin-6; IL-2: interleukin-2; microRNA-19b-3p, miR-19b-3p.

### Rho GTPases Activation Assays

Activation of RhoA was measured by using the Rho Activation Assay Biochem Kit (Cytoskeleton, Denver, CO) according to the manufacturer's instruction. The whole lysates were incubated with Rhotekin-RBD beads for 1 h and washed 3 times with washing buffer. The beads were pelleted by centrifugation and resuspended in SDS loading buffer, and subsequently analyzed by immunoblot analysis.

### Western Blot (WB) Assay

Total proteins were extracted from lung tissues using the RIPA buffer (Solarbio, Beijing, China) in the presence of Protease Inhibitor Cocktail (Solarbio) and Protein Phosphatase Inhibitor (Solarbio), loaded on an SDS-PAGE gel, and electroblotted onto PVDF membrane. The primary antibodies were applied for overnight in 5% BSA at 4°C. WB were analyzed using ImageLab (Bio-Rad, Berkeley, CA). Primary antibodies:  $\beta$ -actin antibody (Abcam, Cambridge, UK); NF- $\kappa$ B p65 (Abcam); p-NF- $\kappa$ B p65 (Abcam); phospho-myosin phosphatase target subunit 1 (p-MYPT1; Abcam); MYPT1 (Abcam); RhoA (Abcam); peroxisome proliferator-activated receptor gamma coactivator 1 alpha (PGC1 $\alpha$ ; Abcam); nicotinamide adenine dinucleotide phosphate oxidase 4 (NOX4; Abcam); intercellular adhesion molecule (ICAM-1; Abcam); transforming growth factor-beta1 (TGF- $\beta$ 1; Abcam); COL3A1 (Abcam); COL1A2 (Abcam).

### Detection of ROS

Lung tissues were homogenized and centrifuged at 5000 rpm/min for 10 min. The supernatant was assayed in accordance with the manufacturer's instructions for the Rat Reactive Oxygen Species Cluster Kit (Mlbio, Shanghai, China). The optical density value for each specimen was determined by a microplate reader at 450

nm (FilterMax F3, Molecular Devices Corporation, San Francisco, CA).

### Immunohistochemical Analysis

After paraffin section was dewaxed and hydrated at room temperature, antigen retrieval was then performed by heat inactivation in citrate buffer (pH 6.0; boiled for 10 minutes). Endogenous peroxidase activity was quenched by immersion in 3% hydrogen peroxide for 10 min. The sections which were added with 50  $\mu$ l of goat serum sealing solution, were put in a wet box for 10 minutes. Then, the sections were incubated with CD45 (Abcam) overnight. After the secondary antibody was incubated at room temperature for 30 minutes, the sections were developed with 3, 3' diaminobenzidine solution. The positive cells was observed using optical microscopy (Olympus, Tokyo, Japan). Secondary antibodies: HRP-linked anti-mouse IgG (Cell Signaling Technology, Beverly, MA); HRP-linked anti-rabbit IgG (Cell Signaling Technology).

### Masson Staining Analysis

Lung tissues were fixed in 10% formalin for 48 h. After paraffin embedding, lung tissues were sectioned into 5- $\mu$ m thickness slices and then was stained with Masson's trichrome (Sigma, St. Louis, MO) following a standard protocol.

### Luciferase Reporter Assay

The target gene of miR-19b-3p was confirmed by 3'-untranslated region (UTR) luciferase, wherein the wide-type (WT, 5'-GUAUAUUGUGAUAAUUUGCACA-3'), and mutant (MU, 5'-GUAUAUUGUGAUAAACGUUAGA-3') 3'-UTR of MYPT1 were cloned into the downstream of a luciferase reporter gene in the pmirGLO vector (Promega, Madison, WI). Cells were co-transfected with luciferase constructs and miR-19b-3p

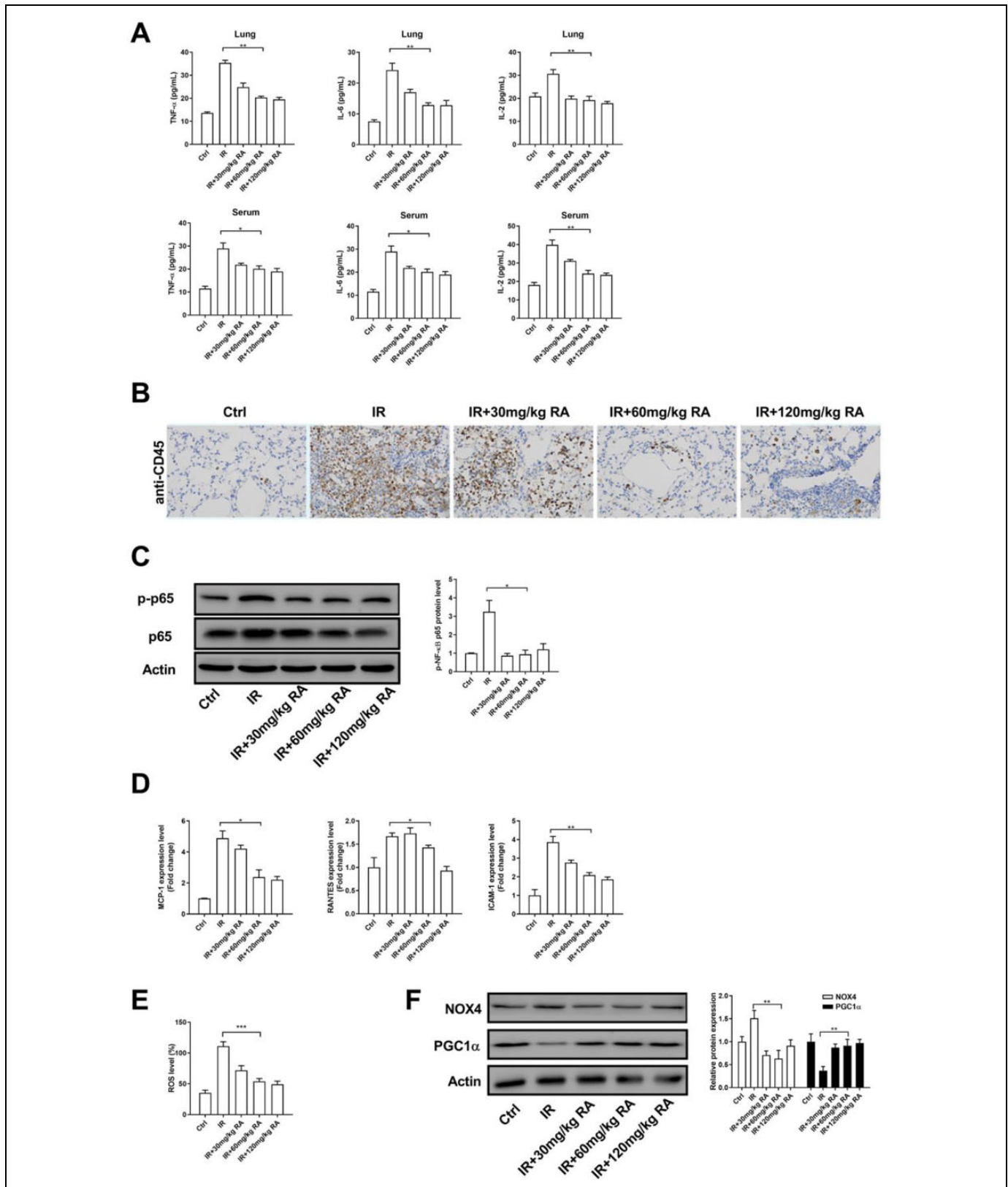


**Figure 2.** RA alleviates inflammation in the lung tissue of IR model rats. A, The expression levels of TNF- $\alpha$ , IL-2, and IL-6 in lung tissue and serum were detected by ELISA assay. B, Example of CD45 staining in the lung tissue of RA-treated rats or controls ( $\times 200$ ). The brown staining represents positive cells. C, The total NF- $\kappa$ B and phosphorylated NF- $\kappa$ B in lung tissue were determined by WB. D, The RNA levels of MCP-1, RANTES, and ICAM-1 in lung tissue were determined by qPCR. E, The ROS levels in lung tissue were determined by ROS assay kit. F, The

mimic. After 48 hours, a dual-luciferase reporter assay system (Promega) system was used to study the luciferase activity.

### Statistical Analysis

The results are expressed as mean  $\pm$  standard error of the mean (SEM) of at least 3 independent experiments. The differences between 2 groups were analyzed by one-way analysis of variance (ANOVA) using SPSS 25.0 (SPSS Inc., Chicago, IL). P-values below 0.05 were considered significantly different.

## Results

### Radiotherapy Results in Inflammatory Reaction and Downregulation of miR-19b-3p

To ascertain the association between miR-19b-3p and IR-induced inflammatory reactions, we first examined the levels of inflammation-related cytokines in the serum of thoracic tumor patients. After radiotherapy treatment, a significant increase of TNF- $\alpha$ , IL-2, and IL-6 was observed compared to the level of these factors before radiotherapy, suggesting that IR induces inflammatory reaction (Figure 1A). We next assessed the expression of miR-19b-3p in the serum of patients. Notably, the miR-19b-3p level was downregulated after radiotherapy (Figure 1B). These data indicate that miR-19b-3p is negatively correlated with the inflammatory reaction.

### Rosmarinic Acid Relieves the X-Ray-Induced Inflammatory Reaction by Downregulating NF- $\kappa$ B and ROS Signaling

To investigate the role of RA in the protective mechanism of inflammation, we assessed the expression levels of TNF- $\alpha$ , IL-2, and IL-6 in lung and serum of IR model rats. Our ELISA results showed that the levels of IL-6, IL-2 and TNF- $\alpha$  increased markedly after X-ray irradiation, which suggested that the local X-ray irradiation of lung initiates the local and systemic inflammatory reaction. Importantly, we observed that RA alleviated inflammation by attenuating the expression of IL-6, IL-2 and TNF- $\alpha$  (Figure 2A). Statistical analysis revealed that the middle dose (60 mg/kg) of RA markedly decreased the expression of inflammation-related factors, whereas higher concentration (120 mg/kg) of RA could not enhance its anti-inflammatory effect, indicating that RA non-dose-dependently (peak effect at 60 mg/kg) mitigated radiation-induced inflammatory reaction. Using immunohistochemical analysis, we observed that the expression of CD45 was sharply reduced in RA-treated groups compared with that in the IR group (Figure 2B). Additionally, RA treatment decreased the

phosphorylation of NF- $\kappa$ B, suggesting that RA attenuated NF- $\kappa$ B signaling in IR model rats (Figure 2C). Consistently, RA treatment reduced RNA levels of NF- $\kappa$ B target gene, including MCP-1, RANTES, and ICAM-1 (Figure 2D). Since the inflammation can accelerate the generation of ROS, we test whether RA affects the ROS level in IR model rats. Indeed, X-ray irradiation elevated the ROS production in lung tissue, whereas treatment with RA led to a decreased in the generation of ROS (Figure 2E). Western blot analysis showed that RA promoted the expression of PGC-1 $\alpha$  and reduced the expression of NOX-4, this evidence further suggested that RA inhibits the generation of ROS (Figure 2F). Together, these results indicate that RA (60 mg/kg) significantly decreased the inflammatory response in the lung.

### Rosmarinic Acid Inhibits Fibrosis in the Lung by Regulating RhoA/Rock Signaling

To further investigate the pharmacological activities of RA, we detected whether RA has anti-fibrotic effects. Masson staining of lung tissue confirmed the increase in ECM deposition in IR model rats and the decrease in ECM deposition with RA treatment (Figure 3A). In line with this observation, pre-administration with RA decreased IR-induced COL3A1 and COL1A2 in lung tissue (Figure 3B). Since the Rho family GTPases have been implicated in the myofibroblast transformation in lung fibrosis, it is reasonable to hypothesize that whether RA treatment affects the activation of GTPases signaling. Indeed, activation of RhoA was observably restrained by RA treatment in IR model rats, as well as the activation of Rock (Figure 3C). In addition, we also found that treatment with RA led to a decreased in the expression of TGF- $\beta$ 1 in lung tissue, a pro-fibrotic cytokine which plays a pivotal role in lung fibrosis (Figure 3D). These data suggest that RA inhibits fibrosis by downregulating RhoA/Rock pathway.

### Rosmarinic Acid Inhibits MYPT1 Expression by Up-Regulating miR-19b-3p

As described thus far, we show that IR reduced the expression of miR-19b-3p, and RA prevents IR-induced inflammation and fibrosis. These observations prompted us to determine the relationship between RA and miR-19b-3p. As shown in Figure 4A, we found that RA treatment enhanced miR-19b-3p expression in IR model rats. To obtain further insight into the function of miR-19b-3p in fibrosis, we performed overexpression and knockdown experiments by transfection with miR-19b-3p mimic or inhibitor in IMR-90 cells. Real-time PCR showed that miR-19b-3p mimic elevated, and miR-19b-3p inhibitor

**Figure 2.** (Continued). protein levels of NOX4 and PGC1 $\alpha$  in lung tissue were determined by WB. (\*P < 0.05; \*\*P < 0.01 in comparison with the indicated group). Abbreviation: TNF- $\alpha$ : Tumor necrosis factor-alpha; IL-6: interleukin-6; IL-2: interleukin-2; NF- $\kappa$ B p65, nuclear factor kappa light chain enhancer of activated B cells p65; MCP-1, monocyte chemo-attractant protein-1; RANTES, regulated upon activation normal T-cell expressed and secreted; ICAM-1, intercellular adhesion molecule-1; ROS, reactive oxygen species; PGC1 $\alpha$ , peroxisome proliferator-activated receptor gamma coactivator-1 alpha; NOX4, nicotinamide adenine dinucleotide phosphatase 4; Ctrl, control; IR, irradiation; RA, rosmarinic acid.

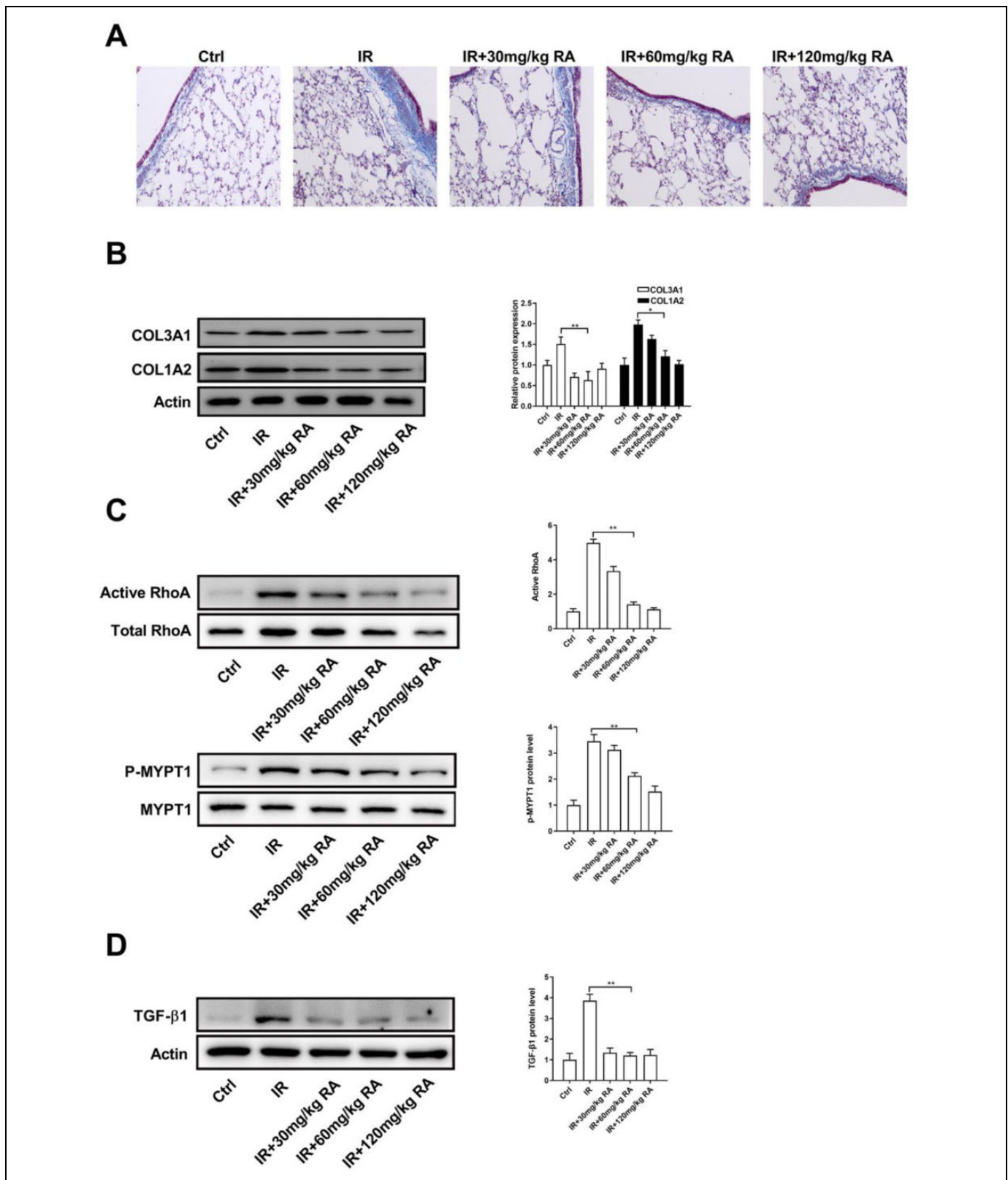


**Figure 3.** RA inhibits RhoA/Rock signaling in the lung tissue of IR model rats. A, Lung tissues of each group were pathologically examined using Masson staining. B, The protein levels of COL3A1 and COL1A2 in lung tissue were determined by WB. C, The total and activated form of RhoA and MYPT1 in lung tissue were determined by WB. D, The protein level of TGF- $\beta$ 1 in lung tissue were determined by WB. (\* $P < 0.05$ ; \*\* $P < 0.01$  in comparison with the indicated group). Abbreviation: p-MYPT1, phospho-myosin phosphatase target subunit 1; TGF- $\beta$ 1, transforming growth factor- $\beta$ 1; Ctrl, control; IR, irradiation; RA, rosmarinic acid.

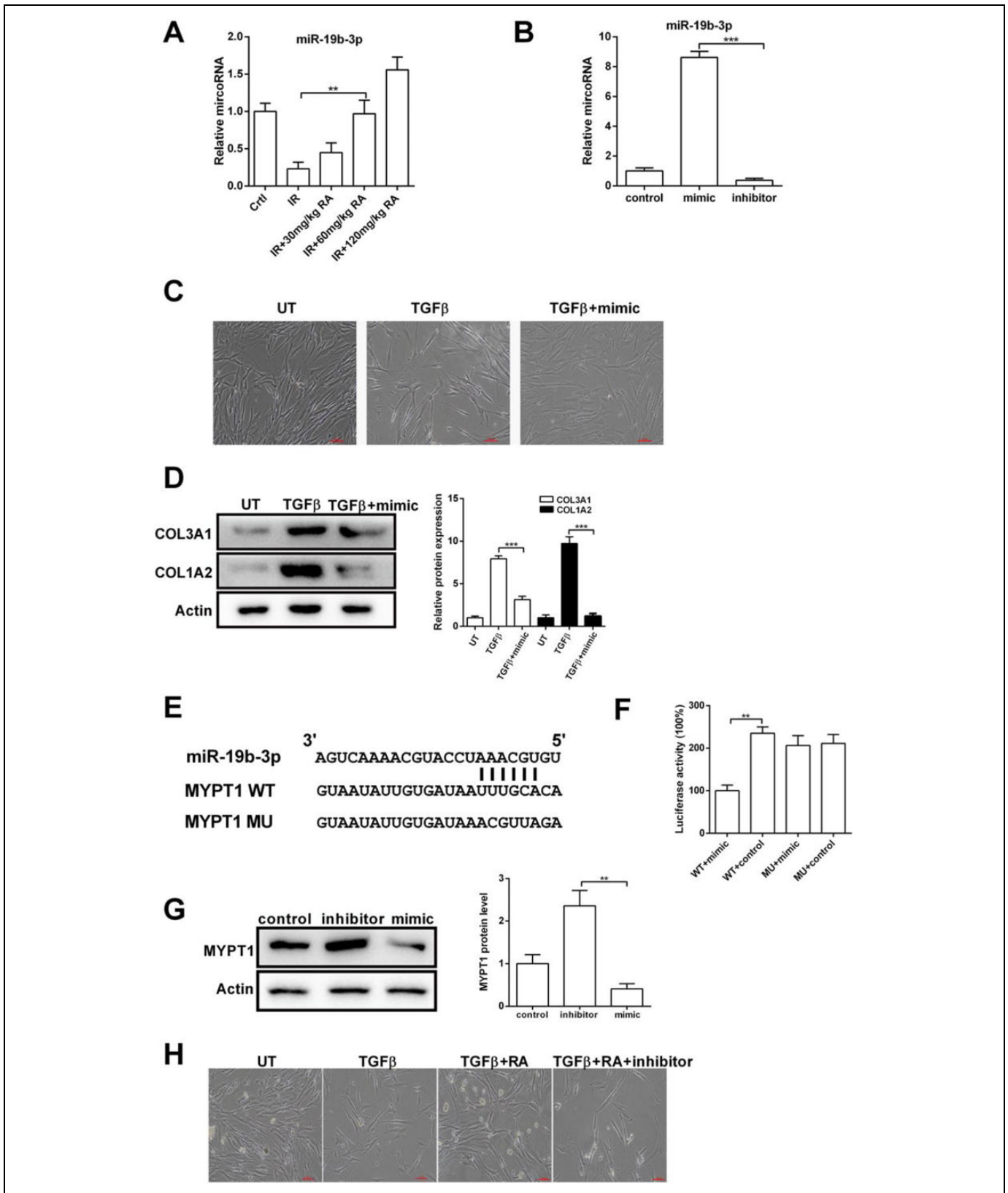


**Figure 4.** RA inhibits TGF $\beta$ -induced fibrosis via miR-19b-3p. **A**, The RNA level of miR-19b-3p in lung tissue was determined by qPCR. **B**, After transfection, the RNA level of miR-19b-3p in IMR-90 cells was determined by qPCR. **C**, IMR-90 cells were treated with or without TGF $\beta$  and miR-19b-3p mimic, and examined under inverted light microscopy. **D**, IMR-90 cells were treated with or without TGF $\beta$  and miR-19b-3p mimic, the protein levels of COL3A1 and COL1A2 were determined by WB. **E**, Graphical representation of the miR-19b-3p binding motif at the MYPT1

reduced the miR-19b-3p expression (Figure 4B). We observed that IMR-90 cells displayed epithelial characteristics under normal conditions, and TGF $\beta$ -treated cells displayed a fibroblastic morphology. Overexpression of miR-19b-3p restored TGF $\beta$ -induced morphological changes, suggesting that miR-19b-3p inhibits fibrosis in IMR-90 cells (Figure 4C). We also found that miR-19b-3p mimic significantly decreased TGF $\beta$ -induced COL3A1 and COL1A2 (Figure 4D). To further explore the relationship between miR-19b-3p and fibrosis, we used bioinformatic analyses and found that miR-19b-3p may target the 3'-UTR of MYPT1 (Figure 4E). Next, we assessed the direct reaction between miR-19b-3p and MYPT1 by dual-luciferase reporter assay. The function of luciferase was inhibited by 58% in cells transfected with miR-19b-3p mimic fused to the 3'-UTR of MYPT1, comparing to the control groups (Figure 4F). We also assessed the expression of MYPT1 by WB in IMR-90 cells after transfection with mimic or inhibitor. MYPT1 protein level was reduced in the mimic presence, while it was significantly enhanced with the inhibitor transfection (Figure 4G). Finally, the effect of RA on TGF $\beta$ -induced fibrosis was attenuated by miR-19b-3p inhibitor (Figure 4H), indicating that RA regulates fibrosis via the miR-19b-3p/MYPT1 axis.

## Discussion

Radiotherapy plays an increasingly prominent role in cancer treatment and has become one of the main methods to treat cancer. However, radiotherapy not only brings survival benefit to patients but also has some toxic side effects. Radiation-induced lung injury is one of the most common and severe complications caused by radiotherapy of the thoracic tumor.<sup>18</sup> The main clinical symptoms of radiation-induced lung injury are inflammatory infiltration of interstitial fluid, progressive dyspnea, deterioration of lung function and respiratory failure.<sup>19</sup> Recently, there is no effective drug for treating radiation-induced lung injury.

Recent studies have emphasized the role of the RA in biological effects, such as anti-inflammatory, anti-diabetes, and anti-cancer activities.<sup>20</sup> Xu et al. reported that RA provides a radio-protective effect against the harmful damage induced by ionizing radiation.<sup>21</sup> However, the underlying mechanism of RA in radiation-induced lung inflammation and pulmonary fibrosis is not entirely clear. Using the rat model, we showed that the expression of IL-6, TNF- $\alpha$  and IL-2 increased significantly after X-ray exposure, which revealed the establishment of inflammation. Notably, administration with RA led to a significant decrease in these inflammatory factors, which are potent stimulants for NK cells to express chemokines.<sup>22</sup> Two

important members of CC-chemokine family, MCP-1 and RANTES, play essential roles in inflammatory cell infiltration, activation, and development of fibrosis. MCP-1 is indispensable for macrophage recruitment and migration. Macrophages secrete interleukin-1 $\beta$ , a growth factor can increase the generation of TGF- $\beta$  and PDGF, eventually leading to fibrosis.<sup>23</sup> Likewise, RANTES and MCP-1 not only contribute to the proliferation and activation of lymphocytes and monocytes/macrophages but also contribute to the secretion of these inflammatory cells, then forming a positive feedback loop.<sup>24</sup> In this study, X-ray irradiation elevated the expression of inflammation marker CD45. Treatment with RA significantly decreased the expression the NOX4, which is constitutively active with hydrogen peroxide (H<sub>2</sub>O<sub>2</sub>) being the primary ROS detectable.<sup>25</sup> Furthermore, RA treatment elevated the expression of PGC-1 $\alpha$ , which counteracted oxidative stress and maintain the expression of antioxidants via suppressing the ROS/FOXO1 signaling axis.<sup>26</sup> Thus, RA attenuated radiation-induced damage by its capacity to relieve inflammation and regulate inflammatory factors. RA reduced the inflammation by attenuating NF- $\kappa$ B signaling. X-ray radiation injury increases the ROS production in lung tissue, and ROS activates the NF- $\kappa$ B pathway.<sup>27,28</sup> NF- $\kappa$ B activation further promotes inflammation.<sup>29,30</sup> Our data showed that RA reduced the NF- $\kappa$ B phosphorylation, as well as the downstream target gene, including ICAM-1, MCP-1, and RANTES. ICAM-1 can strengthen the retention of leukocytes in lung tissue, further intensify the oxidative stress response, and form a vicious circle of oxidative stress inflammatory response.<sup>31,32</sup> It is worth mentioning that RA exerted strongly protective effects in the X-ray-induced inflammation at doses of 60 mg/kg, and treatment with a higher dose (120 mg/kg) do not enhance its anti-inflammatory effect.

It has been reported that RA attenuates airway inflammation by mediating the phosphorylation of ERK, JNK and p38,<sup>33</sup> indicating that RA works by inhibiting the activation of different inflammatory-related pathways. RA suppresses ROS production and lipid peroxidation whereas increases cellular GSH in hepatic stellate cells, meanwhile, down-regulation of Nrf2 abolished RA-mediated inhibition of ROS, indicating that RA regulates intracellular ROS level via the Nrf2 signaling.<sup>34</sup> *In vitro* experiment indicated that a synthesized novel RA derivative (Mito-RA) can use the mitochondrial membrane potential to enter the organelle and protect cells against radiation-induced oxidative injury through scavenging ROS.<sup>35</sup> ROS-induced endothelial stress promotes pericyte differentiate into myofibroblasts via disrupting a normally fine-tuned balance in the Wnt signaling, led to pulmonary fibrosis.<sup>36</sup> We found that RA inhibits X-ray-induced ROS production in lung

**Figure 4.** (Continued). 3'-UTR. F, The luciferase activity displayed by the luciferase reporter constructs which contained either the wild type (WT) or mutation (MU) of human MYPT1 3'-UTR after miR-19b-3p mimic transfection. (\*P < 0.05; \*\*P < 0.01 in comparison with the indicated group). G, WB were performed to evaluate the expression of MYPT1 at the protein levels after transfecting IMR-90 cells with the control, mimic or inhibitor. H, IMR-90 cells were treated with or without TGF $\beta$ , RA, and miR-19b-3p, cell morphology was examined under inverted light microscopy. Abbreviation: microRNA-19b-3p, miR-19b-3p; UT, untreated; TGF- $\beta$ , transforming growth factor-beta; MYPT1, myosin phosphatase target subunit 1; Ctrl, control; IR, irradiation; RA, rosmarinic acid.

tissue, indicating that RA mitigated inflammation and fibrosis by downregulating ROS generation.

Radiation-induced lung injury results in increased phosphorylated MYPT1, indicating that RhoA/Rock pathway is activated in the lung.<sup>37,38</sup> Activation of RhoA/Rock pathway promotes the expression of TGF- $\beta$ 1,<sup>39,40</sup> which plays a pivotal role in pulmonary fibrosis by triggering myofibroblast differentiation, extracellular matrix deposition, and renal epithelial-mesenchymal transition.<sup>41</sup> It is also clear that TGF- $\beta$ 1 promotes the differentiation of fibroblast into myofibroblast via activating a variety of signaling pathways, including the canonical Smad3 pathway and noncanonical pathways, such as PI3K/AKT/mTOR pathway.<sup>42</sup> Elevating TGF- $\beta$  results in increased the expression of Collagen I and Collagen III, and potentiated collagen deposition.<sup>43</sup> Our results demonstrated that the X-ray-induced TGF- $\beta$ 1 was limited in the application of RA. Moreover, RA reduced X-ray-induced accumulation of COL3A1 and COL1A2 after 30 days postirradiation, indicating that RA has a sustained effect on the development of pulmonary fibrosis. MicroRNAs have been implicated in a number of lung diseases, including lung cancer and lung fibrosis. For example, downregulation of let-7 results in epithelial-to-mesenchymal transition and collagen deposition, whereas miR-21 promotes bleomycin-mediated pulmonary fibrosis.<sup>44,45</sup> The miR-19b-3p is involved in the regulation of embryonic fibrosis.<sup>46</sup> However, the functions of miR-19b-3p in irradiation-induced fibrosis remained unclear. In the present study, we found that radiotherapy treatment decreased miR-19b-3p expression in the serum of patients, and overexpression of miR-19b-3p inhibits TGF $\beta$ -induced fibrosis. Furthermore, we confirmed that miR-19b-3p targets MYPT1, suggesting that miR-19b-3p attenuates RhoA/Rock signaling by downregulating MYPT1. Importantly, our results reveal that RA treatment increased the expression of miR-19b-3p, and miR-19b-3p silencing attenuates the anti-fibrotic effect of RA. These observations indicate that RA suppresses RhoA/Rock signaling through elevating miR-19b-3p level.

Previous findings showed that RA attenuates cadmium-induced renal fibrosis by regulating TGF- $\beta$ 1/collagen signaling.<sup>47</sup> RA also regulated epithelial-mesenchymal transition (EMT), a major sources for activated fibroblasts in pulmonary fibrosis, via activating AMP-activated protein kinase (AMPK) in the mouse model.<sup>48</sup> Our results suggest that RA inhibits the development of pulmonary fibrosis via RhoA/TGF- $\beta$ 1/collagen axis.

## Conclusion

In this study, we showed that pre-administration of RA prevents irradiation-induced inflammation by downregulating NF- $\kappa$ B signaling. In addition, RA inhibits RhoA/Rock pathway by upregulating the expression of miR-19b-3p, thus decrease the collagen hyperplasia and inhibit the development of pulmonary fibrosis. Altogether, given its anti-inflammatory and anti-fibrosis effect, RA associated with other drugs may be an

interesting alternative to relieve the pulmonary fibrosis caused by radiotherapy of the thoracic tumor.

## Authors' Note

Tingting Zhang, Shanshan Ma, and Chang Liu contributed equally to this work.

## Declaration of Conflicting Interests

The author(s) declared no potential conflicts of interest with respect to the research, authorship, and/or publication of this article.

## Funding

The author(s) disclosed receipt of the following financial support for the research, authorship, and/or publication of this article: This work was supported by grants from the International Communication of Guangxi Medical University Graduate Education [30/02103009005X], the Basic Ability Enhancement Project of Young Teachers in Guangxi Zhuang Autonomous Region [2019KY0152], the Research Project of Guangxi Health and Family Planning Commission [Z20180925], the Central Guided Local Science and Technology Development Project [GK ZY18076006] and the Guangxi Key Research and Development Plan [GK AD17129013].

## ORCID iD

Tingting Zhang  <https://orcid.org/0000-0001-6286-999X>  
Chang Liu  <https://orcid.org/0000-0002-7047-4901>

## References

1. Kalman NS, Zhao SS, Anscher MS, Urdaneta AI. Current status of targeted radioprotection and radiation injury mitigation and treatment agents: a critical review of the literature. *Int J Radiat Oncol Biol Phys.* 2017;98(3):662-682.
2. Jelonek K, Pietrowska M, Widlak P. Systemic effects of ionizing radiation at the proteome and metabolome levels in the blood of cancer patients treated with radiotherapy: the influence of inflammation and radiation toxicity. *Int J Radiat Biol.* 2017;93(7):683-696.
3. Yilmaz S, Adas YG, Hicsonmez A, Andrieu MN, Akyurek S, Gokce SC. Evaluation of the radiation pneumonia development risk in lung cancer cases. *Asian Pac J Cancer Prev.* 2014;15:7371-7375.
4. He J, Deng L, Na F, Xue J, Gao H, Lu Y. The association between TGF- $\beta$ 1 polymorphisms and radiation pneumonia in lung cancer patients treated with definitive radiotherapy: a meta-analysis. *PLoS One.* 2014;9(3):e91100.
5. Li C, Yu Y, Li W, et al. Phycocyanin attenuates pulmonary fibrosis via the TLR2-MyD88-NF- $\kappa$ B signaling pathway. *Scient Rep.* 2017;7(1):5843.
6. Bei Y, Hua-Huy T, Nicco C, et al. RhoA/Rho-kinase activation promotes lung fibrosis in an animal model of systemic sclerosis. *Exp Lung Res.* 2016;42(1):44-55.
7. Taniguchi K, Karin M. NF- $\kappa$ B, inflammation, immunity and cancer: coming of age. *Natu Rev Immunol.* 2018;18(5):309.
8. Tang H, Gao L, Mao J, et al. Salidroside protects against bleomycin-induced pulmonary fibrosis: activation of Nrf2-antioxidant signaling, and inhibition of NF- $\kappa$ B and TGF- $\beta$ 1/

- Smad-2/-3 pathways. *Cell Stress Chaperones*. 2016;21(2): 239-249.
9. Abdel-Messeih PL, Nosseir NM, Bakhe OH. Evaluation of inflammatory cytokines and oxidative stress markers in prostate cancer patients undergoing curative radiotherapy. *Cent Eur J Immunol*. 2017;42(1):68.
  10. Cikman O, Ozkan A, Aras AB, et al. Radioprotective effects of *Nigella sativa* oil against oxidative stress in liver tissue of rats exposed to total head irradiation. *J Invest Surg*. 2014;27(5): 262-266.
  11. Meng Y, Li T, Zhou G-S, et al. The angiotensin-converting enzyme 2/angiotensin (1-7)/Mas axis protects against lung fibroblast migration and lung fibrosis by inhibiting the NOX4-derived ROS-mediated RhoA/Rho kinase pathway. *Antioxid Redox Signal*. 2015;22(3):241-258.
  12. Bartel DP. MicroRNAs: genomics, biogenesis, mechanism, and function. *Cell*. 2004;116(2):281-297.
  13. Wang L, Yang G, Zhao D, et al. CD103-positive CSC exosome promotes EMT of clear cell renal cell carcinoma: role of remote MiR-19b-3p. *Molecular Cancer*. 2019;18(1):86.
  14. Song M, Sun M, Xia L, Chen W, Yang C. miR-19b-3p promotes human pancreatic cancer Capan-2 cells proliferation by targeting phosphatase and tension homolog. *Ann Translat Med*. 2019;7(11): 236.
  15. Kim G-D, Park YS, Jin Y-H, Park C-S. Production and applications of rosmarinic acid and structurally related compounds. *Appl Microbiol Biotechnol*. 2015;99(5):2083-2092.
  16. Jin B-R, Chung K-S, Cheon S-Y, et al. Rosmarinic acid suppresses colonic inflammation in dextran sulphate sodium (DSS)-induced mice via dual inhibition of NF- $\kappa$ B and STAT3 activation. *Sci Rep*. 2017;7:46252.
  17. Wei Y, Chen J, Hu Y, et al. Rosmarinic acid mitigates lipopolysaccharide-induced neuroinflammatory responses through the inhibition of TLR4 and CD14 expression and NF- $\kappa$ B and NLRP3 inflammasome activation. *Inflammation*. 2018; 41(2):732-740.
  18. Vujaskovic Z, Marks LB, Anscher MS. The physical parameters and molecular events associated with radiation-induced lung toxicity. *Semin Radiat Oncol*. 2000;10(4):296-307.
  19. Han S, Gu F, Lin G, et al. Analysis of clinical and dosimetric factors influencing radiation-induced lung injury in patients with lung cancer. *J Cancer*. 2015;6(11):1172.
  20. Amoah SK, Sandjo LP, Kratz JM, Biavatti MW. Rosmarinic acid—pharmaceutical and clinical aspects. *Planta Med*. 2016; 82(05):388-406.
  21. Xu W, Yang F, Zhang Y, Shen X. Protective effects of rosmarinic acid against radiation-induced damage to the hematopoietic system in mice. *J Radiat Res*. 2016;57(4):356-362.
  22. Peng Y, Kwok K, Yang P-H, et al. Ascorbic acid inhibits ROS production, NF- $\kappa$ B activation and prevents ethanol-induced growth retardation and microencephaly. *Neuropharmacol*. 2005; 48(3):426-434.
  23. Sassy-Prigent C, Heudes D, Mandet C, et al. Early glomerular macrophage recruitment in streptozotocin-induced diabetic rats. *Diabetes*. 2000;49(3):466-475.
  24. Wada T, Furuichi K, Sakai N, et al. Up-regulation of monocyte chemoattractant protein-1 in tubulointerstitial lesions of human diabetic nephropathy. *Kidney Int*. 2000;58(4):1492-1499.
  25. Serrander L, Cartier L, Bedard K, et al. NOX4 activity is determined by mRNA levels and reveals a unique pattern of ROS generation. *Biochem J*. 2007; 406 (1):105-114.
  26. Baldelli S, Aquilano K, Ciriolo MR. PGC-1 $\alpha$  buffers ROS-mediated removal of mitochondria during myogenesis. 2014; 5(11):e1515.
  27. Li D-Z, Zhang Q-X, Dong X-X, et al. Treatment with hydrogen molecules prevents RANKL-induced osteoclast differentiation associated with inhibition of ROS formation and inactivation of MAPK, AKT and NF-kappa B pathways in murine RAW264. 7 cells. *J Bone Mineral Metabol*. 2014;32(5):494-504.
  28. Zhang R, Yin X, Shi H, et al. Adiponectin modulates DCA-induced inflammation via the ROS/NF-kappa B signaling pathway in esophageal adenocarcinoma cells. *Digest Dis Sci*. 2014; 59(1):89-97.
  29. Yan R, Li Y, Zhang L, et al. Augmenter of liver regeneration attenuates inflammation of renal ischemia/reperfusion injury through the NF-kappa B pathway in rats. *Int Urol Nephrol*. 2015;47(5):861-868.
  30. Huang Y, Zeng J, Chen G, et al. Periodontitis contributes to adipose tissue inflammation through the NF- $\kappa$ B, JNK and ERK pathways to promote insulin resistance in a rat model. *Microbes Infect*. 2016;18(12):804-812.
  31. Li Q, Liu BC, Lv LL, et al. Monocytes induce proximal tubular epithelial–mesenchymal transition through NF-kappa B dependent upregulation of ICAM-1. *J Cell Biochem*. 2011;112(6): 1585-1592.
  32. Tang D, Tao D, Fang Y, et al. TNF-alpha promotes invasion and metastasis via NF-kappa B pathway in oral squamous cell carcinoma. *Med Sci Monit Basic Res*. 2017;23:141-149.
  33. Liang Z, Xu Y, Wen X, et al. Rosmarinic acid attenuates airway inflammation and hyperresponsiveness in a murine model of asthma. *Molecules*. 2016;21(6):769.
  34. Lu C, Zou Y, Liu Y, et al. Rosmarinic acid counteracts activation of hepatic stellate cells via inhibiting the ROS-dependent MMP-2 activity: involvement of Nrf2 antioxidant system. *Toxicol Appl Pharmacol*. 2017;318:69-78.
  35. Zhang Y-R, Li Y-y, Wang J-Y, et al. Synthesis and characterization of a rosmarinic acid derivative that targets mitochondria and protects against radiation-induced damage in vitro. *Radiat Res*. 2017;188(3):264-275.
  36. Andersson-Sjöland A, Karlsson JC, Rydell-Törmänen K. ROS-induced endothelial stress contributes to pulmonary fibrosis through pericytes and Wnt signaling. *Lab Invest*. 2016;96(2):206.
  37. MacKay CE, Shaifta Y, Snetkov VV, et al. ROS-dependent activation of RhoA/Rho-kinase in pulmonary artery: role of Src-family kinases and ARHGEF1. *Free Radic Biol Med*. 2017;110: 316-331.
  38. Lu W, Kang J, Hu K, et al. The role of the Nox4-derived ROS-mediated RhoA/Rho kinase pathway in rat hypertension induced by chronic intermittent hypoxia. *Sleep Breath*. 2017;21(3): 667-677.

39. Liu L-J, Yao F-J, Lu G-H, et al. The role of the Rho/ROCK pathway in Ang II and TGF- $\beta$ 1-induced atrial remodeling. *PLoS One*. 2016;11(9):e0161625.
40. Lu A, Zuo C, He Y, et al. EP3 receptor deficiency attenuates pulmonary hypertension through suppression of Rho/TGF- $\beta$ 1 signaling. *J Clin Invest*. 2015;125(3):1228-1242.
41. Jiang HS, Zhu LL, Zhang Z, Chen H, Chen Y, Dai YT. Estradiol attenuates the TGF- $\beta$ 1-induced conversion of primary TAFs into myofibroblasts and inhibits collagen production and myofibroblast contraction by modulating the Smad and Rho/ROCK signaling pathways. *Int J Mol Med*. 2015;36(3):801-807.
42. Biernacka A, Dobaczewski M, Frangogiannis NG. TGF- $\beta$  signaling in fibrosis. *Growth Factors*. 2011;29(5):196-202.
43. Chan KM, Fu SC, Wong YP, et al. Expression of transforming growth factor  $\beta$  isoforms and their roles in tendon healing. *Wound Repair Regen*. 2008;16(3):399-407.
44. Pandit KV, Corcoran D, Yousef H, et al. Inhibition and role of let-7d in idiopathic pulmonary fibrosis. *Am J Respir Crit Care Med*. 2010;182(2):220-229.
45. Liu G, Friggeri A, Yang Y, et al. miR-21 mediates fibrogenic activation of pulmonary fibroblasts and lung fibrosis. *J Exp Med*. 2010;207(8):1589-1597.
46. Chen X, Qu Y, Cheng Y, et al. MiR-19b-3p regulates MAPK1 expression in embryonic fibroblasts from the great tit (parus major) under hypoxic conditions. *Cel Physiol Biochem*. 2018;46(2):546-560.
47. Joardar S, Dewanjee S, Bhowmick S, et al. Rosmarinic acid attenuates cadmium-induced nephrotoxicity via inhibition of oxidative stress, apoptosis, inflammation and fibrosis. *Int J Mol Sci*. 2019;20(8):2027.
48. Han Y-H, Kee J-Y, Hong S-H. Rosmarinic acid activates AMPK to inhibit metastasis of colorectal cancer. *Front Pharmacol*. 2018;9:68.